# Co-ordination Chemistry of Higher Oxidation States. Part 32.[1] Synthetic, Spectroscopic, and Electrochemical Studies of some *trans*-$[OsL_2X_4]$–$[OsL_2X_4]^-$ Systems ($L = PR_3, AsR_3, SbR_3, SeMe_2$, or pyridine; X = Cl or Br). Crystal Structure of $[PPh_4][Os(PEt_3)_2Cl_4]$†

**Robert A. Cipriano, William Levason,* Roy A. S. Mould, Derek Pletcher, and Michael Webster**
*Department of Chemistry, The University, Southampton SO9 5NH*

The preparations of *trans*-$[OsL_2X_4]$ (L = $PEt_3$, $PPh_3$, $PEt_2Ph$, $PEtPh_2$, $AsEt_3$, $AsPh_3$, $SbPh_3$, $SeMe_2$, or pyridine; X = Cl or Br) are described. Reduction of these with ascorbic acid in ethanol in the presence of $PPh_4^+$ or $NEt_4^+$ ions (and in other ways) leads to $[OsL_2X_4]^-$ ions. Both series of complexes were characterised by analysis, i.r., and u.v.–visible spectroscopy, and magnetic measurements. The paramagnetic $[Os(PR_3)_2X_4]$ show sharp $^{31}P$-$\{^1H\}$ n.m.r. resonances with very large low-frequency shifts (*ca.* −1 200 p.p.m.). Assignments are proposed for the major features in the u.v.–visible spectra in terms of intraconfigurational, *d–d*, and ligand-to-metal charge-transfer transitions. Cyclic voltammetry has been used to study the osmium(IV)–osmium(III) couples in these systems, and the redox potentials correlated with the energies of the lowest charge-transfer transitions in the u.v.-visible spectra. The *X*-ray structure of $[PPh_4]$ [*trans*-$Os(PEt_3)_2Cl_4$] has been determined: space group $P2_1/n$ with $a = 12.225(2)$, $b = 17.882(1)$, $c = 18.551(2)$ Å, $\beta = 103.22(1)°$, $Z = 4$; least-squares refinement converged to $R = 0.053$ ($R' = 0.048$). The anion has approximate $D_{4h}$ symmetry with Os–Cl 2.375(3)—2.386(2) Å and Os–P 2.371(3), and 2.386(3) Å.

We have recently reported detailed studies of various iridium(IV) complexes of types *trans*-$[IrL_2X_4]$ and *cis*-$[Ir(L\text{–}L)X_4]$ (L = pyridine, $PR_3$, $AsR_3$, $SbR_3$, $SR_2$, *etc*; L–L = chelating bidentate analogues of L; X = Cl or Br).[2,3] In particular for the iridium(IV) complexes $[IrL_2X_4]$ we observed systematic changes in the spectroscopic and electrochemical properties with changes in L and X (a $d^5$ system). In the present paper we have carried out similar studies on the $d^5$–$d^4$ systems *trans*-$[OsL_2X_4]$–*trans*-$[OsL_2X_4]^-$. Osmium(IV) complexes of the type *trans*-$[OsL_2X_4]$ (L = $PR_3$ or $AsR_3$, X = Cl or Br) are well known,[4–10] but the corresponding osmium(III) anions $[OsL_2X_4]^-$ have been little studied.[10–12] Here we report the syntheses of new examples of the latter, and complexes of osmium(IV) with pyridine, $SeMe_2$, and $SbR_3$.

## Results and Discussion

*Synthesis and Properties.*—Of the various literature routes available,[4,6,10] we find that the osmium(IV) complexes *trans*-$[OsL_2X_4]$, where X = Cl or Br, and L is a phosphine or arsine with one or more alkyl substituents, are best made by reaction of $OsO_4$, L, and concentrated HX in ethanol solution. If these reactions are carried out at low temperatures the osmium(VI) intermediates, *trans*-$[OsO_2L_2X_2]$, can be isolated,[4,13,14] whilst with a larger excess of ligand and more prolonged reaction times osmium(III) complexes $[OsL_3X_3]$ are the major products. Unless carefully controlled this route proves unsatisfactory for $PPh_3$ and $AsPh_3$,[4,13,15] and we find that $[OsL_2X_4]$ (L = $PPh_3$ or $AsPh_3$) are best made by reaction of $OsO_4$, excess of L, and concentrated HX in $Bu^tOH$, followed by treatment with the appropriate halogen in $CHCl_3$ to convert lower oxidation-state osmium complexes which are also present into osmium(IV). The $[Os(SbPh_3)_2X_4]$ are most readily obtained by treatment of *mer*-$[Os(SbPh_3)_3X_3]$ with $X_2$–$CH_2Cl_2$ [the by-product $SbPh_3X_2$ can be isolated from the mother-liquor after crystallisation of the osmium(IV) complex], but several attempts to obtain $SbEt_3$ analogues gave intractable oils. The *trans*-$[Os(SeMe_2)_2X_4]$ complexes were obtained by reaction of $SeMe_2$ and $[OsX_6]^{2-}$ in $Bu^nOH$, but attempts to make analogues with $TeMe_2$ were unsuccessful. As reported previously[16] osmium(IV) complexes of $SMe_2$ have proved elusive, all the more surprising since the osmium(VI) complexes $[OsO_2(SMe_2)_2X_2]$ can be readily obtained from $OsO_4$–HX–$SMe_2$–EtOH.[17] Pyrolysis of $[Hpy]_2[OsX_6]$ (py = pyridine) under nitrogen was explored as a route to $[Os(py)_2X_4]$ {*cf.* the production of $[Os(bipy)Cl_4]$ from $[H_2bipy][OsCl_6]$[18], bipy = 2,2′-bipyridine}, however the crude pale orange products contained osmium(III) rather than osmium(IV) on the basis of their u.v.–visible spectra, and for X = Cl the major product was $[Os(py)_2Cl_4]^-$.[12] The latter was oxidised by $Cl_2$–$CH_2Cl_2$ to purple $[Os(py)_2Cl_4]$, which is also obtained more directly from prolonged reflux of $Na_2[OsCl_6]$ and pyridine (1:2 ratio) in ethanol. The $[Os(py)_2Br_4]$ was obtained by the latter route. When pure the osmium(IV) complexes are deeply coloured yellow-brown to dark red (Cl) or purple (Br) (Table 1), although small changes in the reaction conditions sometimes result in very dark or black materials which have 'extra' absorptions in the visible spectra and 'extra' features in the cyclic voltammograms, and probably contain dinuclear species, *cf.* ref. 19. Reports of black $[OsL_2X_4]$ complexes in the literature, *e.g.* ref. 20, presumably refer to these materials.

The syntheses of the osmium(III) phosphine anions $[OsL_2X_4]^-$ were initially carried out by literature routes, namely reaction of the nitrido complexes $[OsNX_4]^-$ with $PR_3$,[11] whilst $[Os(PEt_3)_2Cl_4]^-$ also arises as a by-product of $NaBH_4$ reduction of $[Os(PEt_3)_2Cl_4]$, *cf.* ref. 10. These reactions do not work for arsines or stibines, but we find that, like $[IrL_2X_4]$,[2] the $[OsL_2X_4]$ are reduced by refluxing with ascorbic acid in

---

† Tetraphenylphosphonium *trans*-tetrachlorobis(triethylphosphine)-osmate(III).

*Supplementary data available:* see Instructions for Authors, *J. Chem. Soc., Dalton Trans.*, 1990, Issue 1, pp. xix—xxii.

*Non-S.I. unit employed:* B.M. ≈ $9.27 \times 10^{-24} Am^2$.

**Table 1.** Selected spectroscopic data for *trans*-$[OsL_2X_4]$ complexes

| | | | $E_{max.}$/10$^3$ cm$^{-1}$ ($\varepsilon$/dm$^3$ mol$^{-1}$ cm$^{-1}$)[a] | | |
|---|---|---|---|---|---|
| Complex | Colour | $\nu$(Os–X)[b]/cm$^{-1}$ | Intraconfigurational[c] + *d–d* | $\sigma_L \longrightarrow Os(t_{2g})$ | $\pi_x \longrightarrow Os(t_{2g})$ |
| $[Os(PEt_3)_2Cl_4]$ | Orange-red | 321 | 4.25, 5.72 | 13.81(1 140) | 21.46(420), 26.11(7 330), 31.45(2 340) |
| $[Os(PEt_2Ph)_2Cl_4]$ | Orange-brown | 320 | 4.24, 6.25 | 13.81(950) | 21.50(950), 24.45(sh), 26.11(5 330), 31.85(sh) |
| $[Os(PEtPh_2)_2Cl_4]$ | Brown | 323 | 4.20, 6.05 | 14.00(940) | 21.83(sh), 25.51(4 730), 31.85(sh) |
| $[Os(PPh_3)_2Cl_4]$ | Dark brown | 323 | 4.20, 5.55 | 14.33(1 030) | 21.83(sh), 25.38(4 390), 30.67(sh) |
| $[Os(PMe_2Ph)_2Cl_4]$ | Brown | 324 | n.m.[d] | 14.30(400) | 20.20(sh), 26.50(4 450) |
| $[Os(AsEt_3)_2Cl_4]$ | Orange | 324 | 4.12, 6.10 | 13.59(1 310) | 21.19(430), 25.00(sh), 26.60(7 690) |
| $[Os(AsPh_3)_2Cl_4]$ | Dark brown | 322 | 4.26, 5.88 | 14.66(800) | 20.24(sh), 22.12(sh), 26.38(5 790) |
| $[Os(SbPh_3)_2Cl_4]$ | Dark red | 322 | 4.27, 5.74 | 11.99(900) | 19.61(680), 26.25(sh), 29.85(30 100), 31.85(24 900) |
| $[Os(py)_2Cl_4]$ | Blue-purple | 306 | n.m. | 18.83(1 230)[e] | 24.27(2 450), 27.03(5 050), 29.67(6 260)[f] |
| $[Os(SeMe_2)_2Cl_4]$ | Green-purple | 310 | n.m. 14.60(sh) | 18.70(290)[e] | 24.20(1 670), 26.60(1 990), 28.60(2 190)[g] |
| $[Os(PEt_3)_2Br_4]$ | Purple | 224 | 4.20, 5.38, 8.72(200) | 12.76(2 375) | 18.45(4 240), 21.41(8 475), 26.67(1 100), 30.30(2 690) |
| $[Os(PPh_3)_2Br_4]$ | Purple | 227 | 4.35, 8.33(400) | 13.46(1 150) | 17.61(5 170), 19.76(sh), 20.45(3 400) |
| $[Os(AsEt_3)_2Br_4]$ | Purple | 223 | 4.35, 8.99(350) | 12.42(2 300) | 18.69(6 180), 21.79(9 680), 26.88(1 100), 30.03(2 910) |
| $[Os(AsPh_3)_2Br_4]$ | Purple | 228 | 4.25, 5.40, 8.77(150) | 13.46(2 480) | 17.73(5 220), 20.49(4 180), 25.58(1 700) |
| $[Os(SbPh_3)_2Br_4]$ | Purple | 232 | 4.25, 8.33(450), 15.50(860) | 10.99(1 480) | 18.02(3 550), 20.90(4 260), 28.82(13 130), 31.85(12 290) |
| $[Os(py)_2Br_4]$ | Purple | 210 | n.m. | | 17.66[h], 20.16, 24.40, 31.01 |
| $[Os(SeMe_2)_2Br_4]$ | Brown-purple | 223 | n.m. | | 16.31(640), 18.08(1 470), 20.96(3 780), 23.47(1 850), 25.84(2 190), 29.50(1 440) |

[a] Dichloromethane solution. [b] Nujol mull. [c] Intensities of intraconfigurational bands not measured due to solvent overtones in the same region. [d] n.m. = Not measured. [e] $\pi_L \longrightarrow Os(t_{2g})$. [f] In MeCN solution. [g] In $Me_2SO$ solution. [h] Poorly soluble, $\varepsilon$ not accurately determined.

ethanol, although the reactions are slower than for the iridium complexes and complicated by the instability of some of the osmium(III) complexes in solution. Despite this, pure osmium(III) complex anions can be obtained. The ascorbic acid reduction also works for the phosphine complexes and appears to be a general route to the osmium(III) anions. Fanwick *et al.*[12] have reported very recently that alkylphosphines cleave the $[Os_2X_8]^{2-}$ ions to yield $[Os(PR_3)_2X_4]^-$, but it is not known if similar reactions occur with arsenic or antimony donors.

The $[OsL_2X_4]$ complexes are stable solids, easily soluble in a wide range of organic solvents. The $[OsL_2X_4]^-$ anions are notably less stable, even the solids slowly darken in air over several months. The stability in solution is dependent upon the solvent, the neutral ligand and halide combination present, and although most of the complexes can be recovered after rapid recrystallisation from concentrated solutions, this instability is much more of a problem in the dilute solutions used for spectroscopic and electrochemical studies. In dichloromethane solution in the presence of air the triphenylphosphine and arsine complexes rapidly develop the characteristic spectra of the corresponding osmium(IV) complexes, but with the trialkylphosphine analogues the reaction is much slower; in neither case does the oxidation appear to go to completion, a mixture of osmium(III) and osmium(IV) usually being present. The air oxidation is not observed for any of the complexes in ethanol or propylene carbonate solution. In rigorously degassed dichloromethane solutions the complexes all show changes in the u.v.–visible spectra with time, which we interpret as indicating rearrangement or disproportionation to other osmium(III) complexes. The reactions are slowest for the phosphine chlorides, more rapid for the phosphine bromides and for the arsines. The triphenylstibine chloro complex is particularly unstable in dilute solution, and on warming an ethanol solution the green *mer*-$[Os(SbPh_3)_3Cl_3]$ precipitates, and a stibine-free red solution remains probably largely hexachloro-osmate(IV) from the spectrum. Curiously the corresponding $[Os(SbPh_3)_2Br_4]^-$ is relatively stable in solution. The decomposition of the osmium(III) anions in solution is also evident in the electrochemical studies (below).

Conductivities of the osmium(III) anions in freshly prepared MeCN solution are consistent with 1:1 electrolytes ($\Lambda_M$ = 100—120 ohm$^{-1}$ cm$^2$ mol$^{-1}$).[21] The *trans*-$[OsL_2X_4]$ complexes have magnetic moments $\mu$ 1.4—1.6 B.M. in the solid state at ambient temperature, whilst those of the osmium(III) anions $[OsL_2X_4]^-$ are rather greater $\mu$ 1.8—2.0 B.M. The values are consistent with theoretical predictions[22] for $5d_{t_{2g}}{}^4$ and $5d_{t_{2g}}{}^5$ configurations, and with previously reported values for osmium(IV) and osmium(III) complexes.[6,8] The $[Os(PR_2Ph)_2Cl_4]$ (R = Bu$^n$ or Pr$^n$) were reported to give sharp $^{31}$P n.m.r. resonances[7] with very large low-frequency shifts due to the paramagnetism. Similar shifts have been found for $PEt_3$, $PEt_2Ph$, $PEtPh_2$, and $PPh_3$ complexes (Table 3), with the resonances of the bromides being slightly to low frequency of the chlorides. As expected no $^{31}$P n.m.r. resonances were observed for the osmium(III) complexes.

*trans* Octahedral structures were assigned to all the $[OsL_2X_4]^{0/-}$ species on the basis of the single Os–X stretching vibration in the far-i.r. spectrum of each (Tables 1 and 2) and from the similarity of the u.v.–visible spectra within each series. Confirmation of the geometry is provided by *X*-ray crystallographic data on $[Os(PMe_2Ph)_2Cl_4]$,[9] $[Os(AsPh_3)_2Br_4]$,[23] and $[PPh_4][Os(PEt_3)_2Cl_4]$ (below).

*X-Ray Structure of* $[PPh_4][Os(PEt_3)_2Cl_4]$.—The structure consists of discrete *trans*-$[Os(PEt_3)_2Cl_4]^-$ anions (see Figure 1) and tetraphenylphosphonium cations, and selected distances and angles are shown in Table 4. The anion has no crystallographic symmetry but the $OsP_2Cl_4$ residue is close to $D_{4h}$ symmetry. Several metal(IV) *trans*-$[M(PR_3)_2X_4]$ structures have been reported for M = Os,[9] Re,[24] Ta,[25] Pt,[9,26] and others,

**Table 2.** Selected spectroscopic data for $[ER_4][OsL_2X_4]$ complexes

| Complex | Colour | ν(Os–X)[a]/cm$^{-1}$ | $E_{max.}/10^3$ cm$^{-1}$ (ε/dm$^3$ cm$^{-1}$ mol$^{-1}$)[b] |
|---|---|---|---|
| $[PPh_4][Os(PEt_3)_2Cl_4]$ | Yellow | 290 | 4.24, 7.05, 21.74(600),[c] 26.32(sh), 27.93(470), 31.45(4 435) |
| $[PPh_4][Os(PEt_2Ph)_2Cl_4]$ | Yellow | 290 | 4.20, 7.14, 22.12(680),[c] 27.47(sh), 30.86(5 675), 31.25(sh) |
| $[PPh_4][Os(PEtPh_2)_2Cl_4]$ | Yellow | 296 | 4.20, 22.32(990),[c] 27.78(sh), 31.55(5 270) |
| $[PPh_4][Os(PPh_3)_2Cl_4]$ | Yellow | 294 | 4.25, 7.46, 22.83(720),[c] 26.45(sh), 30.12(5 750) |
| $[AsPh_4][Os(AsPh_3)_2Cl_4]$ | Brown | 313 | n.m. 21.90(700)(sh),[c] 25.90(2 050), 30.12(sh)(5 500) |
| $[AsPh_4][Os(SbPh_3)_2Cl_4]$ | Brown | 317 | 4.40, 6.25, 18.05(1 830),[c] 21.93(990), 24.75(sh), 27.70(3 760), 29.40(3 000)[d] |
| $[PPh_4][Os(PEt_3)_2Br_4]$ | Orange | 211 | 5.13, 11.11(sh), 17.42(500), 19.05(1 860),[e] 19.76(sh), 20.16(4 470), 23.03(8 090), 23.70(4 160), 24.40(sh)[f] |
| $[PPh_4][Os(PEt_2Ph)_2Br_4]$ | Orange | 210 | 4.40, 5.18, 11.36(sh), 17.45(680), 19.01(1 910),[e] 19.76(sh), 20.20(4 320), 22.20(5 830), 23.92(3 750), 24.27(3 570)[f] |
| $[PPh_4][Os(PPh_3)_2Br_4]$ | Orange | 215 | 4.40, 6.89, 17.67(sh), 18.90(sh)[e], 20.12(2 330), 22.73(3 060), 25.68(1 980) |
| $[NEt_4][Os(AsEt_3)_2Br_4]$ | Brown | 216 | n.m. 17.48(690), 19.08(2 410)[e], 19.92(sh), 20.28(6 140), 22.17(9 490), 23.92(5 590), 24.51(sh)[d] |
| $[PPh_4][Os(AsPh_3)_2Br_4]$ | Brown | 206 | n.m. 17.70(890), 20.66(2 320), 23.31(3 880), 26.18(2 410) |
| $[NEt_4][Os(SbPh_3)_2Br_4]$ | Red-brown | 208 | 4.40, 5.10, 6.66, 14.95(110), 18.18(1 250)[e], 20.20(1 190), 22.27(1 650), 23.64(3 560), 26.53(1 190)[d] |

[a] Nujol mull. [b] Dichloromethane solution unless indicated otherwise. [c] $\sigma_L \longrightarrow Os(t_{2g})$ see text. [d] In MeCN solution. [e] Possibly $\sigma_L \longrightarrow Os(t_{2g})$ see text. [f] Ethanol solution.

**Table 3.** $^{31}P-\{^1H\}$ N.m.r. data for $[Os(PR_3)_2X_4]$ (δ/p.p.m.)*

| | | | |
|---|---|---|---|
| $[Os(PEt_3)_2Cl_4]$ | −1 211 | $[Os(PEtPh_2)_2Cl_4]$ | −1 191 |
| $[Os(PEt_3)_2Br_4]$ | −1 237 | $[Os(PPh_3)_2Cl_4]$ | −1 199 |
| $[Os(PEt_2Ph)_2Cl_4]$ | −1 196 | $[Os(PPh_3)_2Br_4]$ | −1 220 |

* In $CH_2Cl_2$ solution relative to 85% $H_3PO_4$, high frequency positive convention.

but little data are available on the corresponding metal(III) anions. On a small sample there appears to be a trend in the Os-Cl (*trans* Cl) distances with the osmium oxidation state, the higher the oxidation state the shorter is the bond.

$Os^V$–Cl 2.284(av.) in $[PPh_4][OsCl_6]$[27] [2.252(4)–2.295(2)Å]
$Os^{IV}$–Cl 2.332(av.) in $[PPh_4]_2[OsCl_6]$[27] [2.325(3)–2.338(3)Å]
2.319(av.) in $[Os(PMe_2Ph)_2Cl_4]$[9]
$Os^{III}$–Cl 2.380(av.) in present compound
2.347 in *mer*-$[Os(PMe_2Ph)_3Cl_3]$[9]

A large number of complexes containing the triethylphosphine ligand have been examined by *X*-ray diffraction[28] and the ligand geometry in the present compound seems unexceptional. The stereochemical problem of fitting a ligand of three-fold symmetry onto an acceptor ($MX_4$) with four-fold symmetry seems to be solved in a similar way for many of the complexes. One of the XMPC torsion angles is close to 45° with the corresponding MPCC torsion angle about 180°. That is C(5)C(6) and C(9)C(10) in the present example. The other two ethyl groups adopt a staggered conformation with respect to the P–C bond (*gauche* to both the first P–C bond and the M–P bond), *e.g.* C(5)P(1)C(1)C(2) is −57° giving the $PEt_3$ residue an idealised $C_s$ symmetry. In the present compound only the ligand involving P(1) adopts this conformation whereas in $[M(PEt_3)_2Cl_4]$ (M = Re or Ta) both the phosphorus ligands adopt it and indeed are related by a crystallographic centre of symmetry located on M. The triethylarsine ligand in $[Ir(AsEt_3)_2Br_4]$ is also very similar.[2] The conformation of $[PPh_4]^+$ has been discussed extensively[29,30] but in the present compound inspection of the torsion angles established that the cation did not approximate to $D_{2d}$, $D_2$, or $S_4$ symmetry.

*U.V.–Visible Spectra.*—$[OsL_2X_4]$. The data are listed in Table 1 and typical spectra are shown in Figure 2. The assignments are based upon a $t_{2g}^4$ ground state and comparisons with $[OsX_6]^{2-}$.[31,32] All complexes show weak

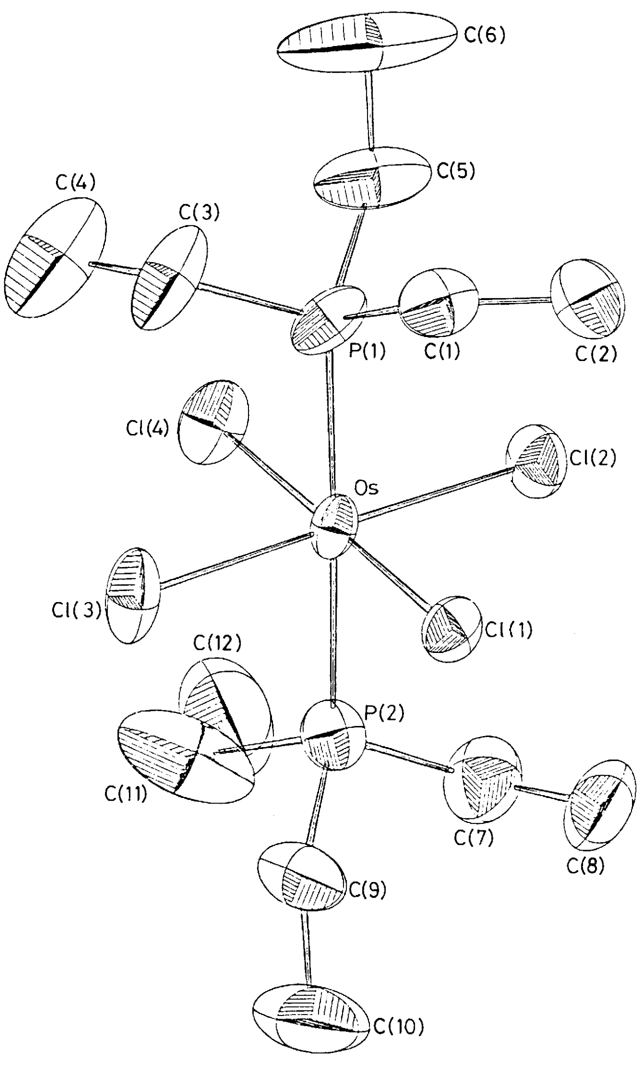

**Figure 1.** View of the anion *trans*-$[Os(PEt_3)_2Cl_4]^-$ showing the atom numbering scheme. Thermal ellipsoids are drawn with 40% probability surfaces and H-atom positions are omitted for clarity

**Table 4.** Selected bond lengths (Å) and angles (°) for $[PPh_4][Os(PEt_3)_2Cl_4]$

| | | | | | | | |
|---|---|---|---|---|---|---|---|
| Os–Cl(1) | 2.386(2) | P(1)–C(1) | 1.84(1) | P(3)–C(21) | 1.787(8) | C(1)–C(2) | 1.53(2) |
| Os–Cl(2) | 2.376(2) | P(1)–C(3) | 1.84(1) | P(3)–C(31) | 1.788(8) | C(3)–C(4) | 1.48(2) |
| Os–Cl(3) | 2.375(3) | P(1)–C(5) | 1.83(1) | P(3)–C(41) | 1.792(8) | C(5)–C(6) | 1.52(2) |
| Os–Cl(4) | 2.385(2) | P(2)–C(7) | 1.82(1) | P(3)–C(51) | 1.794(9) | C(7)–C(8) | 1.52(2) |
| Os–P(1) | 2.371(3) | P(2)–C(9) | 1.82(1) | | | C(9)–C(10) | 1.56(2) |
| Os–P(2) | 2.386(3) | P(2)–C(11) | 1.93(2) | Cl . . . P(min.) | 3.26 | C(11)–C(12) | 1.40(2) |

C–C (phenyl) min. 1.33(1) max. 1.43(1) mean 1.38(2)

| | | | | | | | |
|---|---|---|---|---|---|---|---|
| Cl(1)–Os–Cl(2) | 91.3(1) | P(2)–Os–Cl(1) | 89.5(1) | Os–P(2)–C(9) | 113.3(4) | P(2)–C(11)–C(12) | 107.8(15) |
| Cl(1)–Os–Cl(3) | 89.4(1) | P(2)–Os–Cl(2) | 92.1(1) | Os–P(2)–C(11) | 113.8(6) | C(1)–P(1)–C(3) | 99.7(5) |
| Cl(2)–Os–Cl(4) | 89.9(1) | P(2)–Os–Cl(3) | 86.4(1) | P(1)–C(1)–C(2) | 114.3(8) | C(3)–P(1)–C(5) | 106.1(6) |
| Cl(3)–Os–Cl(4) | 89.5(1) | P(2)–Os–Cl(4) | 91.4(1) | P(1)–C(3)–C(4) | 116.7(10) | C(5)–P(1)–C(1) | 103.8(6) |
| P(1)–Os–Cl(1) | 91.2(1) | Os–P(1)–C(1) | 117.2(4) | P(1)–C(5)–C(6) | 116.7(10) | C(7)–P(2)–C(9) | 104.9(6) |
| P(1)–Os–Cl(2) | 89.4(1) | Os–P(1)–C(3) | 115.1(5) | P(2)–C(7)–C(8) | 111.9(9) | C(9)–P(2)–C(11) | 98.2(6) |
| P(1)–Os–Cl(3) | 91.1(1) | Os–P(1)–C(5) | 113.3(4) | P(2)–C(9)–C(10) | 118.2(10) | C(11)–P(2)–C(7) | 107.7(8) |
| P(1)–Os–Cl(4) | 88.0(1) | Os–P(2)–C(7) | 117.0(4) | | | | |

| | | |
|---|---|---|
| C–P(3)–C | min. 107.4(4) | max. 111.9(4) |
| C–C–C | min. 119(1) | max. 121(1) |

| | | | |
|---|---|---|---|
| Os–P(1)–C(1)–C(2) | 69 | Os–P(2)–C(7)–C(8) | 67 |
| Os–P(1)–C(3)–C(4) | −64 | Os–P(2)–C(9)–C(10) | −175 |
| Os–P(1)–C(5)–C(6) | 178 | Os–P(2)–C(11)–C(12) | 95 |
| Cl(1)–Os–P(1)–C(1) | 13 | Cl(1)–Os–P(2)–C(7) | −81 |
| Cl(2)–Os–P(1)–C(5) | 43 | Cl(1)–Os–P(2)–C(9) | 41 |
| C(5)–P(1)–C(1)–C(2) | −57 | C(9)–P(2)–C(7)–C(8) | −60 |
| C(5)–P(1)–C(3)–C(4) | 62 | C(9)–P(2)–C(11)–C(12) | −145 |

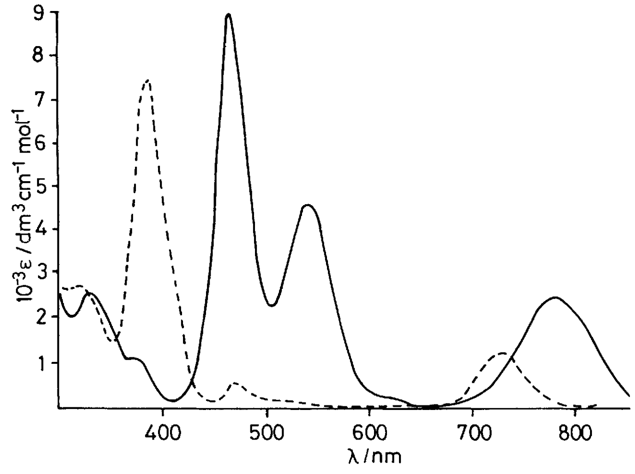

**Figure 2.** U.v.–visible spectra of *trans*-$[Os(PEt_3)_2Cl_4]$ (– – –) and *trans*-$[Os(PEt_3)_2Br_4]$(——)in $CH_2Cl_2$ solution

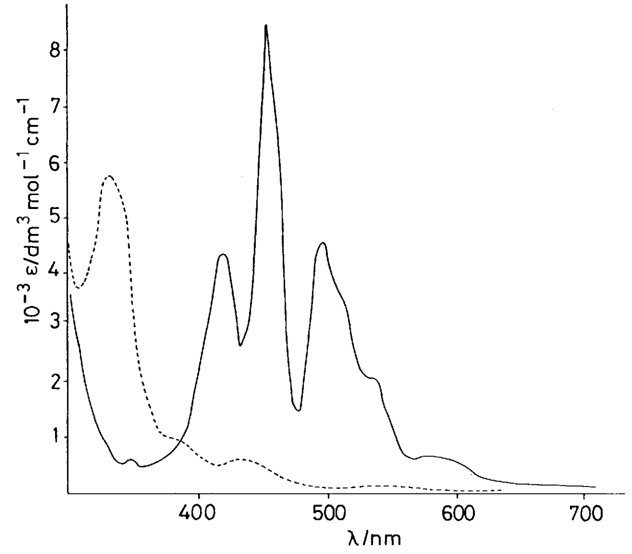

**Figure 3.** U.v.–visible spectra of $[PPh_4][Os(PPh_3)_2Cl_4]$ (– – – –) and $[PPh_4][Os(PEt_3)_2Br_4]$ (——) in deoxygenated $CH_2Cl_2$ solution

features in the region 4 000—6 000 cm$^{-1}$ which are intra-configurational bands, and intense absorptions > *ca.* 10 000 cm$^{-1}$ which are expected to be mainly L $\longrightarrow$ Os charge-transfer (c.t.) transitions.[2] In $D_{4h}$ symmetry the $\sigma_L$, $\sigma_X$, and $\pi_X$ orbitals are not strongly mixed, and assignments of transitions from these individual orbitals to Os($t_{2g}$) are reasonable. For the low-spin $5d_{t_{2g}}^{4}$ ions, with the exception of $[OsF_6]^{2-}$, *d–d* transitions are usually obscured by the more intense charge-transfer bands.[32] In $[OsCl_6]^{2-}$ the allowed $\pi_{Cl} \longrightarrow$ Os($t_{2g}$) c.t. transitions lie in the range 26 000—30 000 cm$^{-1}$, with the corresponding $\pi_{Br} \longrightarrow$ Os($t_{2g}$) in $[OsBr_6]^{2-}$ at 17 000—25 000 cm$^{-1}$. The assignment of the strong bands at 24 000—32 000 cm$^{-1}$ in $[OsL_2Cl_4]$ and 17 000—27 000 cm$^{-1}$ in $[OsL_2Br_4]$ as $\pi_X \longrightarrow$ Os($t_{2g}$) follows by analogy. The intense single absorptions of each complex with P, As, or Sb donor atoms at *ca.* 11 000—15 000 cm$^{-1}$ which vary in energy with L are assigned as $\sigma_L \longrightarrow$ Os($t_{2g}$), and it is notable that for fixed L the energy of this transition is somewhat lower in the bromides than in the chlorides. For $[OsL'_2X_4]$ (L′ = $SeMe_2$ or py) bands at 18 700 and 18 500 cm$^{-1}$ respectively are assigned as $\pi_{L'} \longrightarrow$ Os($t_{2g}$) charge transfer, the larger transition energy reflecting the lower energy of the π orbitals in these ligands.[2] For $[OsL'_2Br_4]$ assignment of the transition from $\pi_L$ is more difficult since the lower $\pi_{Br} \longrightarrow$ Os transitions occur at similar energies. Weaker features at *ca.* 21 000 cm$^{-1}$ for the chlorides and at *ca.* 9 000 cm$^{-1}$ for the bromides are less readily assigned. That at 21 000 cm$^{-1}$ could be a parity-forbidden $\pi_{Cl} \longrightarrow$ Os($t_{2g}$) transition, but its separation in energy from the other

**Table 5.** Cyclic voltammetry data[a] for the osmium complexes $[OsL_2X_4]^{0/-}$

| | X = Cl | | X = Br | |
|---|---|---|---|---|
| L | *b* | *c* | *b* | *c* |
| $PEt_3$ | 0.33 | 0.32 | 0.37 | *d* |
| $PEt_2Ph$ | 0.36 | 0.36 | | |
| $PEtPh_2$ | 0.43 | 0.41 | | |
| $PPh_3$ | 0.47 | 0.48 | 0.49 | 0.47 |
| $AsEt_3$ | 0.27 | | 0.33 | *d* |
| $AsPh_3$ | 0.48 | 0.48 | 0.54 | 0.52 |
| $SbPh_3$ | 0.51 | | 0.56 | 0.56 |
| py | 0.47 | | 0.52 | |
| $SeMe_2$ | 0.48 | | 0.50 | |

[a] Formal potentials *vs.* the standard calomel electrode (s.c.e.) for the couples $[OsL_2X_4]$–$[OsL_2X_4]^-$ in $CH_2Cl_2$ containing 0.2 mol $dm^{-3}$ $[NBu^n{}_4]BF_4$. Potential of $[Fe(\eta\text{–}C_5H_5)_2]$–$[Fe(\eta\text{–}C_5H_5)_2]^+$ is 0.57 V *vs.* s.c.e. under these conditions. Potential scan rates 0.025—0.2 V $s^{-1}$. $E_p{}^A - E_p{}^C$ fell in the range 60—80 mV. [b] Voltammograms recorded with *ca.* 1.0 mmol $dm^{-3}$ $[OsL_2X_4]$ solution. [c] Voltammograms recorded with *ca.* 1.0 mmol $dm^{-3}$ $[OsL_2X_4]^-$ solution. [d] Solution of the complex decomposes too rapidly to obtain reliable data.

$\pi_{Cl} \longrightarrow$ Os bands appears rather large. The band at 9 000 $cm^{-1}$ present for all the bromides must be of *d–d* type, and is probably related (in $O_h$ symmetry) to the $^3T_{1g}(\Gamma^1) \longrightarrow {}^1T_{1g}$, $^1E_g$ band observed at 10 900 $cm^{-1}$ for $[OsBr_6]^{2-}$.[31]

$[OsL_2X_4]^-$. The spectra are listed in Table 2 and Figure 3 shows typical examples. The spectra of $[OsX_6]^{3-}$ have been little studied,[32] but an early paper by Jorgensen[33] identified the $\pi_X \longrightarrow Os(t_{2g})$ at $\geqslant$ 32 000 (X = Cl) and $\geqslant$ 22 000 $cm^{-1}$ (X = Br). In view of the instability of the osmium(III) anions in solution referred to above, obtaining reliable spectroscopic data proved to be quite difficult. All solution spectra were run immediately after the solutions were made up, and in the cases of those complexes which showed rapid oxidation to osmium(IV) the solutions were made up on a vacuum line using cells fitted with Teflon taps. The spectral data reported in Table 3 are believed to be correct despite these instability problems, since there is generally a good correspondence between them and the diffuse reflectance spectra of the solid complexes. Generally spectra were also recorded after allowing the solutions to stand, and after deliberately exposing them to air, which allowed the band(s) formed by oxidation or decomposition to be identified.

For $[OsL_2Cl_4]^-$ the strong band(s) and associated shoulders which lie $\geqslant$29 000 $cm^{-1}$ are assigned as $\pi_{Cl} \longrightarrow Os(t_{2g})$ c.t. transitions, with the single strong feature at *ca.* 22 000 $cm^{-1}$ as $\sigma_L \longrightarrow Os(t_{2g})$. The spectra of the $[OsL_2Br_4]^-$ are much richer, probably reflecting the increased splitting produced by the greater spin–orbit coupling constant of bromine, and their assignment is complicated by the fact that the $\sigma_L \longrightarrow Os(t_{2g})$ and $\pi_{Br} \longrightarrow Os(t_{2g})$ are now of similar energy. The tentative assignment of the bands in Table 2 indicated as possible $\sigma_L \longrightarrow Os(t_{2g})$ transitions were made after comparison both of the spectra of different $[OsL_2Br_4]^-$ and with their $[OsL_2Cl_4]^-$ analogues, but in view of the complications outlined above are less certain than for the other complexes. The spectra of $[OsL_2X_4]^-$ can be compared with those of the isoelectronic $[IrL_2X_4]^2$ for which $\sigma_L \longrightarrow Ir(t_{2g})$ were found at *ca.* 8 000—10 000, $\pi_{Cl} \longrightarrow Ir(t_{2g})$ 17 000—20 000, and $\pi_{Br} \longrightarrow Ir(t_{2g})$ 13 000—16 000 $cm^{-1}$. Such a comparison shows that between osmium(III) and iridium(IV) the $\sigma_L \longrightarrow M(t_{2g})$ c.t. bands are shifted by 12 000—14 000 $cm^{-1}$, the $\pi_{Cl} \longrightarrow M(t_{2g})$ by *ca.* 10 000 $cm^{-1}$, and $\pi_{Br} \longrightarrow M(t_{2g})$ by *ca.* 7 000 $cm^{-1}$. Although the ligands clearly exert some mutual influence on the metal centres, the greater relative magnitude of the shift in $\sigma_L \longrightarrow$ M c.t. band is consistent with a weaker interaction between the metal and the soft Group 5B donor in the higher oxidation state, and is supported by the trends in M–P bond lengths between $[Os(PEt_3)_2Cl_4]^-$ and $[Ir(PMe_2Ph)_2Cl_4]$[9] [Os–P 2.378(av.), Ir–P 2.392 Å]. Comparison of the $d^4$ osmium(IV) and the $d^5$ osmium(III) complexes is complicated in that a different spin-pairing correction is necessary (4/3*D* and 2/3*D* respectively),[32] and unfortunately values for the ligand-field parameters necessary to make such a correction are generally not available for heavy-metal ions, since the *d–d* transitions are usually obscured by c.t. bands. The energies of the lowest $\sigma_L \longrightarrow$ M c.t. bands $Ir^{IV} < Os^{IV} < Os^{III}$ do however reflect the relative oxidising power of the complexes.

*Electrochemistry.*—Cyclic voltammetry was used to investigate the $Os^{IV}$–$Os^{III}$ couples in each of the $[OsL_2X_4]$ and $[OsL_2X_4]^-$ complexes synthesised during this programme. The experiments used a polished vitreous carbon electrode and $CH_2Cl_2$–$[NBu^n{}_4]BF_4$ as the medium and *I vs. E* curves were recorded at several potential scan rates in the range 0.05—0.4 V $s^{-1}$; potentials are reported relative to the standard calomel electrode.

With one exception, cyclic voltammograms for the $[OsL_2X_4]$ complexes run between 1.0 and 0.0 V were straightforward. In each case a single reduction process was observed and the voltammograms had the form expected for a reversible one-electron transfer process.[34] A typical set for *trans*-$[Os(PPh_3)_2Br_4]$ is shown in Figure 4. The formal potentials for the $Os^{IV}$–$Os^{III}$ couples, taken from the average of the forward and reverse peak potentials, are reported in Table 5. Voltammograms were also recorded with the negative potential limit extended to $-1.5$ V. For several complexes, additional reduction processes were observed but the number of peaks, their potentials, and the relative size of the peaks depended strongly upon the nature of L and X. In the absence of a single pattern of behaviour, these further reduction processes were not studied in detail. The voltammetry of $[Os(SbPh_3)_2Cl_4]$ showed an additional complication. Although at high potential scan rates (> 1 V $s^{-1}$) it is also reduced in a reversible one-electron process, below 0.2 V $s^{-1}$ the coupled anodic peak at $+0.54$ V is much diminished in height and a new oxidation peak is seen on the reverse scan at $+0.65$ V; clearly the anion $[Os(SbPh_3)_2Cl_4]^-$ is not stable on the time-scale of more than a few seconds in this solution.

If the $[OsL_2X_4]^-$ complexes were completely stable, it is to be expected that the voltammograms run between 0.0 and $+1.0$ V would be identical to those obtained for $[OsL_2X_4]$ except for a shift with respect to the zero current line. Such behaviour was indeed observed for some complexes, see for example Figure 4. The formal potentials for the $Os^{IV}$–$Os^{III}$ couples taken from such curves are reported in Table 5. Of course, the values obtained from experiments with corresponding $[OsL_2X_4]$ and $[OsL_2X_4]^-$ solutions should be the same, and this appears to be the case within experimental error. However with some anions, *e.g.* $[Os(PPh_3)_2Br_4]^-$, the cyclic voltammograms were found to change with time; the peaks for the reversible one-electron oxidation decrease in height and a new irreversible oxidation peak at more positive potential grows with time (see Figure 4). With other complexes, namely $[Os(AsEt_3)_2Br_4]^-$ and $[Os(PEt_3)_2Br_4]^-$ this decomposition was so rapid that it was not possible to observe the reversible $Os^{III}$–$Os^{IV}$ couple. In practice cyclic voltammetry proved to be a reliable and rapid way to demonstrate the solution stability of the $[OsL_2X_4]^-$ complexes. In general the decomposition is slowest for X = Cl and L = $PPh_3$ or $AsPh_3$; replacement of Cl by Br, or Ph by Et, increased the decomposition rates {the pair $[Os(SbPh_3)_2Cl_4]^-$ and $[Os(SbPh_3)_2Br_4]^-$ seem to be the exception}.

The formal potentials in Table 5 are consistent with the half-wave potentials reported earlier[11,12] for the oxidation of

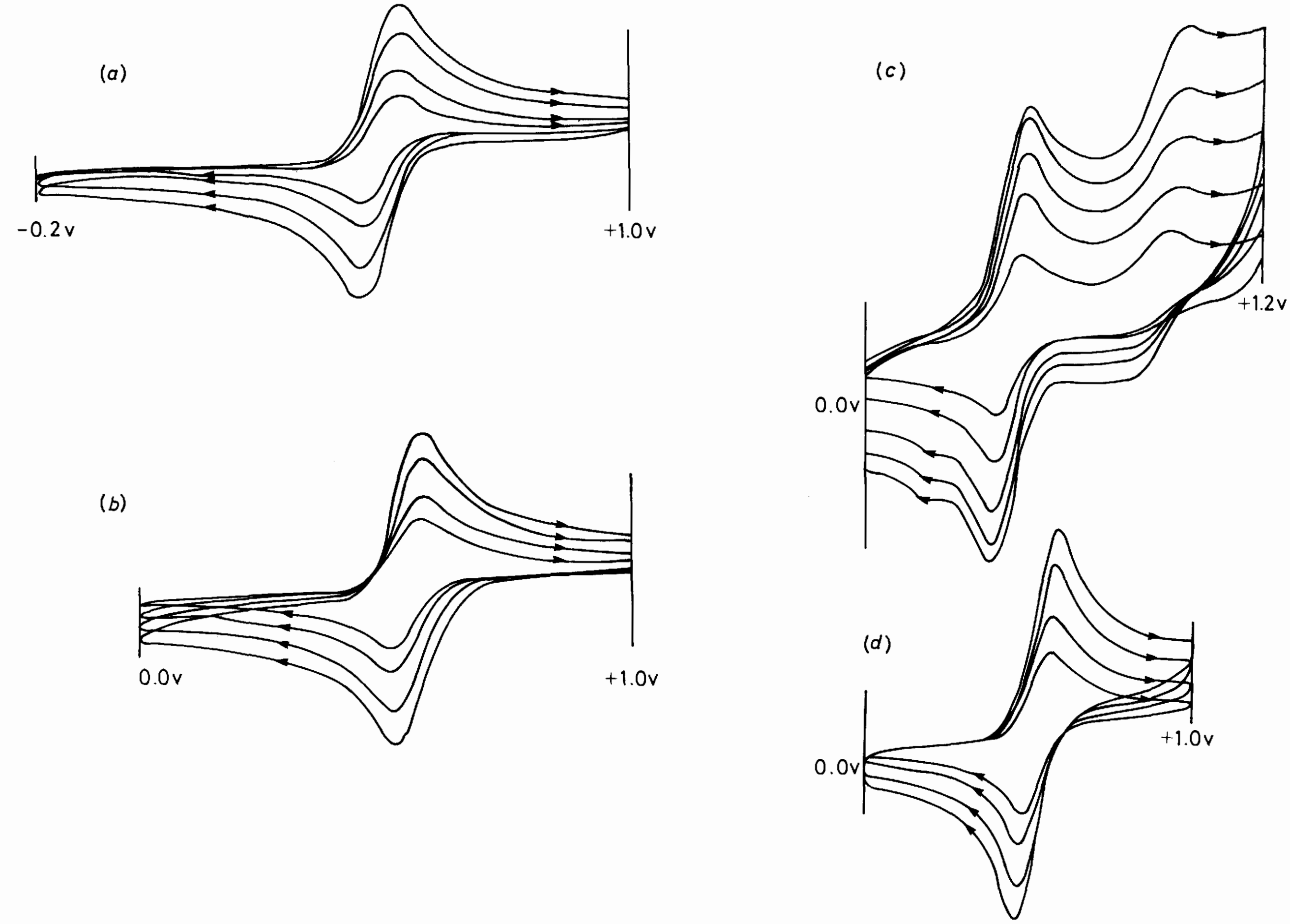

**Figure 4.** Cyclic voltammograms for (*a*) $[Os(PPh_3)_2Br_4]$, (*b*) $[Os(AsPh_3)_2Br_4]$, (*c*) $[PPh_4][Os(PPh_3)_2Br_4]$, and (*d*) $[PPh_4][Os(AsPh_3)_2Br_4]$, all at a vitreous carbon electrode in $CH_2Cl_2$–$[NBu^n{}_4]BF_4$

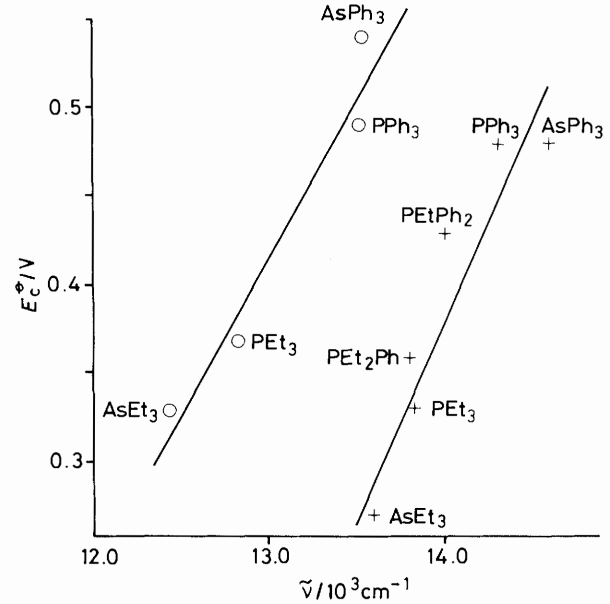

**Figure 5.** Dependence of the formal electrode potential on the energy of the $\sigma_L \longrightarrow Os(t_{2g})$ c.t. transition for $[OsL_2X_4]$. X = Br(O) or Cl(+)

$[Os(PEt_3)_2X_4]^-$. It is also apparent that the trends in formal potential are very similar to those found previously for the corresponding iridium complexes.[2] Thus, for example, the potential shifts positive along the series with L = $PR_3$ as ethyl groups are replaced by phenyls, while the replacement of Cl by Br has little effect upon the formal potentials of the couples.

We have previously observed[2] that in the $[IrL_2X_4]$–$[IrL_2X_4]^-$ systems a plot of the formal potential $Ir^{IV}$–$Ir^{III}$ *versus* the energy of the $\sigma_L \longrightarrow$ Ir c.t. transition energy gave a linear regression. Similarly the plots of the formal $Os^{IV}$–$Os^{III}$ potentials *versus* the $\sigma_L \longrightarrow$ Os c.t. transition energies are essentially linear for osmium(IV) compounds of phosphine and arsine ligands, and for similar chloride complexes of osmium(III). An example is shown in Figure 5. The correlation was not attempted for the osmium(III) bromo anions due to the overlap of $\sigma_L \longrightarrow$ Os and $\pi_{Br} \longrightarrow$ Os c.t. bands. As observed for the iridium systems, the stibine complexes and complexes with ligands having low-lying orbitals of π symmetry (py and $SeMe_2$ in the present case) deviate markedly from the regressions for the other compounds.

## Experimental

Physical measurements were made as described in previous parts of this series.[1–3] Osmium tetraoxide and sodium hexachloro-osmate(IV) were obtained from Johnson Matthey Ltd. and used as received. Sodium hexabromo-osmate(IV) was made by repeatedly evaporating $Na_2[OsCl_6]$ to dryness with aqueous HBr. Electrochemical measurements were made as described previously.[2]

*Preparations.*—trans-$[OsL_2X_4]$ (L = $PEt_3$, $PEt_2Ph$, PEt-

$Ph_2$, *or* $AsEt_3$; X = Cl *or* Br). Osmium tetraoxide (0.2 g, 0.8 mmol) was added to a nitrogen-purged mixture of concentrated HX (2 $cm^3$) and ethanol (30 $cm^3$). To the stirred mixture, the ligand (2.4 mmol) was added and the mixture refluxed for several hours. The solution was cooled, concentrated to *ca.* 10 $cm^3$, and stored at 0 °C for several days. The crystalline product was filtered off, washed with a small amount of diethyl ether, and dried *in vacuo*. Yields 40—70%. $[Os(PEt_3)_2Cl_4]$ (Found: C, 25.2; H, 5.3. $C_{12}H_{30}Cl_4OsP_2$ requires C, 25.4; H, 5.3%), $\mu$ = 1.5 B.M.; $[Os(PEt_3)_2Br_4]$ (Found: C, 19.5; H, 4.0. $C_{12}H_{30}Br_4OsP_2$ requires C, 19.3; H, 4.0%), $\mu$ = 1.6 B.M.; $[Os(PEt_2Ph)_2Cl_4]$ (Found: C, 36.1; H, 4.5. $C_{20}H_{30}Cl_4OsP_2$ requires C, 36.2; H, 4.5%), $\mu$ = 1.5 B.M.; $[Os(PEtPh_2)_2Cl_4]$ (Found: C, 44.0; H, 3.9. $C_{28}H_{30}Cl_4OsP_2$ requires C, 44.2; H, 3.9%), $\mu$ = 1.7 B.M.; $[Os(AsEt_3)_2Cl_4]$ (Found: C, 22.0; H, 4.6. $C_{12}H_{30}As_2Cl_4Os$ requires C, 22.0; H, 4.6%), $\mu$ = 1.4 B.M.; $[Os(AsEt_3)_2Br_4]$ (Found: C, 17.1; H, 3.6. $C_{12}H_{30}As_2Br_4Os$ requires C, 17.2; H, 3.6%).

trans-$[OsL_2X_4]$ (L = $PPh_3$ *or* $AsPh_3$, X = Cl *or* Br). Osmium tetraoxide (0.26 g, 1.0 mmol) was added to a thoroughly nitrogen-purged mixture of concentrated HX (3 $cm^3$) and $Bu^tOH$ (25 $cm^3$). The ligand (4.8 mmol) in warm $Bu^tOH$ (8 $cm^3$) was added and the dark mixture refluxed for 2 h. The solution was cooled to room temperature, and filtered. The brown product was washed with ethanol and diethyl ether and dried. It was dissolved in $CHCl_3$ (40 $cm^3$) and a small excess (2 mmol) of the appropriate halogen added in $CHCl_3$. After a few minutes the solution was filtered and dry ethanol (200 $cm^3$) added to precipitate the product. The crystals were rinsed with ethanol and dried *in vacuo*. Yield 40—70%: $[Os(PPh_3)_2Cl_4]$ (Found: C, 50.8; H, 3.6. $C_{36}H_{30}Cl_4OsP_2$ requires C, 50.5; H, 3.5%), $[Os(PPh_3)_2Br_4]$ (Found: C, 41.6; H, 2.9. $C_{36}H_{30}Br_4OsP_2$ requires C, 41.8; H, 2.9%), $[Os(AsPh_3)_2Cl_4]$ (Found: C, 46.0; H, 3.2. $C_{36}H_{30}As_2Cl_4Os$ requires C, 45.8; H, 3.2%), $\mu$ = 1.4 B.M.; $[Os(AsPh_3)_2Br_4]$ (Found: C, 38.3; H, 2.6. $C_{36}H_{30}As_2Br_4Os$ requires C, 38.5; H, 2.7%), $\mu$ = 1.5 B.M.

trans-$[Os(SbPh_3)_2Cl_4]$. The complex $[Os(SbPh_3)_3Cl_3]$[35] (0.21 g, 0.15 mmol) was treated with $CHCl_3$ (20 $cm^3$) saturated with chlorine, forming a deep red solution, which was concentrated on a rotary evaporator to *ca.* 5 $cm^3$. Diethyl ether (150 $cm^3$) was added to precipitate dark red crystals, which were filtered off, rinsed with ether (20 $cm^3$), and dried *in vacuo* (0.11 g, 72%) (Found: C, 41.7; H, 3.0. $C_{36}H_{30}Cl_4OsSb_2$ requires C, 41.6; H, 2.9%), $\mu$ = 1.5 B.M.

trans-$[Os(SbPh_3)_2Br_4]$. Osmium tetraoxide (0.22 g, 0.85 mmol) was added to 47% aqueous HBr (5 $cm^3$) in $Bu^tOH$ (20 $cm^3$), triphenylantimony (1.4 g, 4.0 mmol) in $Bu^tOH$ (20 $cm^3$) added, and the mixture refluxed for 2 h. The mixture was cooled and the grey product $[Os(SbPh_3)_3Br_3]$ filtered off and dried *in vacuo*. The product (0.4 g) was dissolved in dichloromethane (20 $cm^3$) and bromine in $CH_2Cl_2$ (1 $cm^3$ in 20 $cm^3$) added, and the mixture shaken for 2 min. The solution was evaporated under reduced pressure to *ca.* 5 $cm^3$, diethyl ether (20 $cm^3$) added, and the mixture allowed to stand at −10 °C. The purple product was rinsed with diethyl ether (5 $cm^3$) and dried *in vacuo* (0.15 g, 46%) (Found: C, 36.0; H, 2.6. $C_{36}H_{30}Br_4OsSb_2$ requires C, 35.5; H, 2.5%), $\mu$ = 1.5 B.M.

trans-$[Os(SeMe_2)_2X_4]$. A solution of $Na_2[OsX_6]$ (0.8 mmol) in warm n-butanol (15 $cm^3$) was treated with $SeMe_2$ (1.6 mmol), the mixture heated to reflux, and then cooled. The solution was concentrated *in vacuo* to a small volume and treated with diethyl ether to precipitate the product, which was filtered off and dried *in vacuo*. Yield 20% $[Os(SeMe_2)_2Cl_4]$ (Found: C, 9.0; H, 2.1. $C_4H_{12}Cl_4OsSe_2$ requires C, 8.7; H, 2.2%), $[Os(SeMe_2)_2Br_4]$ (Found: C, 6.8; H, 1.8. $C_4H_{12}Br_4OsSe_2$ requires C, 6.6; H, 1.6%).

trans-$[Os(py)_2X_4]$. A solution of $Na_2[OsX_6]$ (0.7 mmol) in ethanol (15 $cm^3$) and pyridine (1.4 mmol) was stirred briefly at room temperature, and then heated to reflux for 3 h. The solution was refrigerated for 48 h, and the solid which deposited, was filtered off, rinsed with ethanol, and dried *in vacuo*. Yield *ca.* 40%: $[Os(py)_2Cl_4]$ (Found: C, 24.2; H, 2.1; N, 5.5. $C_{10}H_{10}Cl_4N_2Os$ requires C, 24.5; H, 2.0; N, 5.7%), $[Os(py)_2Br_4]$ (Found: C, 18.4; H, 1.5; N, 4.0. $C_{10}H_{10}Br_4N_2Os$ requires C, 18.0; H, 1.5; N, 4.2%).

$[PPh_4][Os(PEt_3)_2Cl_4]$. A stirred suspension of $[Os(PEt_3)_2Cl_4]$ (0.25 g, 0.44 mmol) in ethanol (10 $cm^3$) was treated with $NaBH_4$ (0.19 g, 5.1 mmol) and the mixture warmed until the complex had dissolved. The solvent was removed *in vacuo*, and the residue extracted with benzene. The benzene-insoluble residue was extracted with water (10 $cm^3$) giving a yellow solution which on addition of a saturated solution of $PPh_4Cl$ (0.13 g) in water gave yellow crystals (0.25 g, 64%) (Found: C, 48.0; H, 5.4. $C_{36}H_{50}Cl_4OsP_3$ requires C, 47.6; H, 5.5%).

$[PPh_4][OsL_2Cl_4]$ (L = $PEt_2Ph$, $PEtPh_2$, *or* $PPh_3$). The nitrido complex $[PPh_4][OsNCl_4]$[36] (0.22 g, 0.32 mmol) was dissolved in acetone (3 $cm^3$), and L (2 mmol) in acetone (5 $cm^3$) added with stirring. The resulting yellow crystalline product was filtered off, washed with ethanol (5 $cm^3$), and dried *in vacuo*. Yields 20—45%: $[PPh_4][Os(PEt_2Ph)_2Cl_4]$ (Found: C, 52.8; H, 5.0. $C_{44}H_{50}Cl_4OsP_3$ requires C, 52.6; H, 5.0%), $\mu$ = 2.0 B.M.; $[PPh_4][Os(PEtPh_2)_2Cl_4]$ (Found: C, 56.5; H, 4.4. $C_{52}H_{50}Cl_4OsP_3$ requires C, 56.8; H, 4.5%), $\mu$ = 1.9 B.M.; $[PPh_4][Os(PPh_3)_2Cl_4]$ (Found: C, 60.1; H, 4.2. $C_{60}H_{50}Cl_4OsP_3$ requires C, 60.2; H, 4.2%).

$[PPh_4][OsL_2Br_4]$ (L = $PEt_3$, $PEt_2Ph$, *or* $PPh_3$). These salts were prepared similarly to the chlorides, starting from $[PPh_4][OsNBr_4]$.[36] Yields 15—40%: $[PPh_4][Os(PEt_3)_2Br_4]$ (Found: C, 39.6; H, 4.8. $C_{36}H_{50}Br_4OsP_3$ requires C, 39.6; H, 4.6%); $[PPh_4][Os(PEt_2Ph)_2Br_4]$ (Found: C, 45.2; H, 4.2. $C_{44}H_{50}Br_4OsP_3$ requires C, 44.7; H, 4.2%), $\mu$ = 1.8 B.M.; $[PPh_4][Os(PPh_3)_2Br_4]$ (Found: C, 52.3; H, 3.7. $C_{60}H_{50}Br_4OsP_3$ requires C, 52.4; H, 3.6%).

$[AsPh_4][Os(AsPh_3)_2Cl_4]$. The complex $[Os(AsPh_3)_2Cl_4]$ (0.4 mmol) and ascorbic acid (0.45 mmol) were dissolved in ethanol (30 $cm^3$), and excess (*ca.* 1 mmol) of $AsPh_4Cl$ added. The solution was heated to reflux under nitrogen for 0.5 h, cooled, and concentrated under reduced pressure until solid began to separate. The solution was then refrigerated for several hours, the precipitate filtered off, rinsed with ethanol, and dried *in vacuo*. Yield 50% (Found: C, 53.9; H, 3.7. $C_{60}H_{50}As_3Cl_4Os$ requires C, 54.2; H, 3.8%). The salt $[PPh_4][Os(AsPh_3)_2Br_4]$ was made similarly (Found: C, 49.8; H, 3.5. $C_{60}H_{50}As_2OsP$ requires C, 49.3; H, 3.4%).

$[AsPh_4][Os(SbPh_3)_2Cl_4]$. The preparation of the stibine complex was similar, except that after ascorbic acid reduction the solution was filtered to remove green solid *mer*-$[Os(SbPh_3)_3Cl_3]$ (*ca.* 40%), concentrated *in vacuo*, and the required complex precipitated with diethyl ether. Yield *ca.* 15% (Found: C, 50.9; H, 3.6. $C_{60}H_{50}AsCl_4OsSb_2$ requires C, 50.7; H, 3.5%).

$[NEt_4][OsL_2Br_4]$ (L = $AsEt_3$ *or* $SbPh_3$). These salts were made similarly to the chlorides, but using $NEt_4Br$ in place of $AsPh_4Cl$. Yields 25—70%: $[NEt_4][Os(AsEt_3)_2Br_4]$ (Found: C, 25.0; H, 5.3; N, 1.3. $C_{20}H_{50}As_2Br_4NOs$ requires C, 24.9; H, 5.2; N, 1.4%), $\mu$ = 1.8 B.M.; $[NEt_4][Os(SbPh_3)_2Br_4]$ (Found: C, 40.1; H, 3.7; N, 0.9. $C_{44}H_{50}Br_4NOsSb_2$ requires C, 39.3; H, 3.7; N, 1.0%).

X-*Ray Structure Determination*.—Dark yellow air-stable needle crystals of $[PPh_4][Os(PEt_3)_2Cl_4]$ were obtained from ethanol–hexane by vapour diffusion and the density measured by flotation ($CCl_4$–$Et_2O$). Preliminary photographic examination established the crystal system and approximate cell dimensions.

*Crystal data.* $C_{36}H_{50}Cl_4OsP_3$, $M$ = 907.7, monoclinic, $a$ = 12.225(2), $b$ = 17.882(1), $c$ = 18.551(2) Å, $\beta$ = 103.22(1)°, $U$ =

**Table 6.** Atomic co-ordinates for $[PPh_4][Os(PEt_3)_2Cl_4]$

| Atom | $x$ | $y$ | $z$ | Atom | $x$ | $y$ | $z$ |
|---|---|---|---|---|---|---|---|
| Os | 0.111 06(3) | 0.128 45(2) | 0.297 82(2) | C(23) | 0.242 2(8) | −0.104 8(5) | 1.011 3(5) |
| Cl(1) | 0.264 8(2) | 0.115 2(1) | 0.239 4(1) | C(24) | 0.173 5(9) | −0.086 3(6) | 1.057 0(6) |
| Cl(2) | 0.208 9(2) | 0.221 6(1) | 0.378 9(1) | C(25) | 0.137 9(9) | −0.014 8(6) | 1.061 2(6) |
| Cl(3) | 0.009 4(2) | 0.038 0(2) | 0.215 2(2) | C(26) | 0.173 7(8) | 0.041 2(6) | 1.019 2(5) |
| Cl(4) | −0.043 4(2) | 0.138 3(1) | 0.355 9(2) | C(31) | 0.407 1(7) | 0.147 0(4) | 0.995 4(4) |
| P(1) | 0.187 4(3) | 0.035 8(1) | 0.386 5(2) | C(32) | 0.476 5(8) | 0.199 2(5) | 0.971 8(5) |
| P(2) | 0.030 0(2) | 0.219 4(2) | 0.207 2(2) | C(33) | 0.549 3(9) | 0.241 9(6) | 1.023 1(6) |
| P(3) | 0.303 6(2) | 0.097 3(1) | 0.929 0(1) | C(34) | 0.551 8(10) | 0.234 3(6) | 1.096 5(7) |
| C(1) | 0.334 5(9) | 0.007 8(6) | 0.392 8(6) | C(35) | 0.486 9(10) | 0.181 5(6) | 1.121 4(7) |
| C(2) | 0.421 0(10) | 0.068 3(7) | 0.423 9(7) | C(36) | 0.413 6(9) | 0.138 0(6) | 1.069 7(5) |
| C(3) | 0.118 8(10) | −0.056 6(6) | 0.370 9(9) | C(41) | 0.362 4(7) | 0.054 8(5) | 0.858 9(5) |
| C(4) | −0.000 5(15) | −0.060 3(9) | 0.375 4(11) | C(42) | 0.478 3(8) | 0.052 6(5) | 0.864 5(5) |
| C(5) | 0.185 1(12) | 0.062 4(7) | 0.481 5(6) | C(43) | 0.519 5(9) | 0.016 1(5) | 0.810 6(5) |
| C(6) | 0.229 0(18) | 0.005 1(13) | 0.541 5(9) | C(44) | 0.448 7(9) | −0.019 6(6) | 0.753 3(6) |
| C(7) | 0.084 1(11) | 0.314 3(6) | 0.221 7(8) | C(45) | 0.333 5(9) | −0.019 2(6) | 0.747 8(6) |
| C(8) | 0.205 3(12) | 0.319 5(7) | 0.214 8(9) | C(46) | 0.291 1(9) | 0.019 3(5) | 0.800 3(5) |
| C(9) | 0.042 2(12) | 0.195 3(7) | 0.114 3(6) | C(51) | 0.195 0(7) | 0.162 5(5) | 0.889 2(5) |
| C(10) | 0.001 9(16) | 0.253 3(10) | 0.051 4(8) | C(52) | 0.093 9(9) | 0.136 2(6) | 0.853 1(6) |
| C(11) | −0.131 4(13) | 0.224 6(11) | 0.188 3(8) | C(53) | 0.006 9(10) | 0.186 6(6) | 0.819 2(6) |
| C(12) | −0.159 4(17) | 0.281 4(13) | 0.232 7(11) | C(54) | 0.022 9(10) | 0.260 1(6) | 0.828 0(6) |
| C(21) | 0.245 0(7) | 0.024 2(5) | 0.974 0(4) | C(55) | 0.123 8(10) | 0.287 4(7) | 0.865 3(7) |
| C(22) | 0.280 2(7) | −0.049 3(5) | 0.969 7(5) | C(56) | 0.210 8(10) | 0.239 1(6) | 0.897 3(6) |

3 947.9 Å$^3$, $Z = 4$, $D_m = 1.51(2)$, $D_c = 1.527$ g cm$^{-3}$, $F(000) = 1\,820$, space group $P2_1/n$ (no. 14), $\lambda(\text{Mo-}K_\alpha) = 0.7106\,9$ Å, $\mu(\text{Mo-}K_\alpha) = 36.0$ cm$^{-1}$.

Accurate cell dimensions were obtained from 25 reflections recorded on an Enraf–Nonius CAD4 diffractometer equipped with molybdenum radiation and a graphite monochromator. The intensities of 7 542 reflections ($\omega$—$2\theta$ scan, $1.5 < \theta < 25°$; $h$ 0—14, $k$ 0—21, $l$ −22 to +22) were measured from a room-temperature crystal (0.5 × 0.15 × 0.1 mm) using molybdenum radiation. An empirical psi-scan absorption correction (transmission maximum 99.7, minimum 87.6) and Lorentz and polarisation corrections were applied; the check reflections (two) showed no change during the experiment. After data reduction there remained 6 930 unique reflections ($R_{\text{int.}} = 0.021$) and after eliminating those with $F < 3\sigma(F)$ (2 631) there remained 4 299 observed reflections to be used in the analysis and refinement.

The osmium atom was located from the Patterson function and repeated structure-factor and difference electron-density syntheses readily located the remaining non-hydrogen atoms. Later electron-density syntheses showed some of the H atoms and all were introduced into the model in calculated positions [$d$(C–H) = 0.95 Å]. Methyl H atoms were placed in the staggered conformation with a fixed thermal parameter and all other H atoms were given a common refined thermal parameter. Full-matrix least-squares refinement minimising $\Sigma w\Delta^2$ reduced $R$ to 0.053 ($R' = 0.048$) {278 parameters, anisotropic [Os, Cl, P, C(ethyl)] and isotropic [C(phenyl), H] atoms, $w^{-1} = [\sigma^2(F) + 0.0002\,F^2]$, maximum shift/error = 0.18}. A final difference electron-density map showed features in the range 1.47 to −1.21 e Å$^{-3}$ with the largest peak close to the osmium atom.

All calculations were performed on an IBM3090 computer using the SHELX,[37] XANADU,[38] and ORTEP[39] programs. Scattering factors for neutral atoms and anomalous dispersion corrections were taken from SHELX or ref. 40. (Osmium only.) The atomic co-ordinates are given in Table 6.

Additional material available from the Cambridge Crystallographic Data Centre comprises H-atom co-ordinates, thermal parameters, and remaining bond lengths and angles.

## Acknowledgements

We thank the S.E.R.C. for support, Professor M. B. Hursthouse for the *X*-ray data collection on the S.E.R.C./Q.M.C. instrument, and Dow Chemicals Ltd. for leave of absence for postgraduate studies (to R. A. C.).

## References

1 Part 31, L. R. Hanton, W. Levason, and N. A. Powell, *Inorg. Chim. Acta*, 1989, **160**, 205.

2 R. A. Cipriano, W. Levason, D. Pletcher, N. A. Powell, and M. Webster, *J. Chem. Soc., Dalton Trans.*, 1987, 1901.

3 R. A. Cipriano, L. R. Hanton, W. Levason, D. Pletcher, N. A. Powell, and M. Webster, *J. Chem. Soc., Dalton Trans.*, 1988, 2483.

4 J. E. Armstrong and R. A. Walton, *Inorg. Chem.*, 1983, **22**, 1545.

5 J. Chatt, G. J. Leigh, and D. M. P. Mingos, *J. Chem. Soc. A*, 1969, 1674.

6 J. Chatt, G. J. Leigh, D. M. P. Mingos, and R. J. Paske, *J. Chem. Soc. A*, 1968, 2636.

7 E. W. Randall and D. Shaw, *J. Chem. Soc. A*, 1969, 2807.

8 G. J. Leigh and D. M. P. Mingos, *J. Chem. Soc. A*, 1970, 587.

9 L. Aslanov, R. Mason, A. G. Wheeler, and P. O. Whimp, *Chem. Commun.*, 1970, 30.

10 P. G. Douglas and B. L. Shaw, *J. Chem. Soc. A*, 1970, 334.

11 D. Pawson and W. P. Griffith, *J. Chem. Soc., Dalton Trans.*, 1975, 417.

12 P. E. Fanwick, I. F. Fraser, S. M. Tetrick, and R. A. Walton, *Inorg. Chem.*, 1987, **26**, 3786.

13 D. J. Salmon and R. A. Walton, *Inorg. Chem.*, 1978, **17**, 2379.

14 S. K. Harbron and W. Levason, *J. Chem. Soc., Dalton Trans.*, 1987, 633.

15 G. V. Goeden and B. L. Haymore, *Inorg. Chim. Acta*, 1983, **71**, 239.

16 D. J. Gulliver, W. Levason, K. G. Smith, M. J. Selwood, and S. G. Murray, *J. Chem. Soc., Dalton Trans.*, 1980, 1872.

17 S. K. Harbron and W. Levason, *J. Chem. Soc., Dalton Trans.*, 1985, 205.

18 E. M. Kober, J. V. Caspar, B. P. Sullivan, and T. J. Meyer, *Inorg. Chem.*, 1988, **27**, 4587.

19 R. Contreras, G. G. Elliott, R. O. Gould, G. A. Heath, A. J. Lindsay, and T. A. Stephenson, *J. Organomet. Chem.*, 1981, **215**, C6.

20 M. M. T. Khan, S. S. Ahamad, and R. A. Levenson, *J. Inorg. Nucl. Chem.*, 1976, **38**, 1135.

21 W. J. Geary, *Coord. Chem. Rev.*, 1971, **7**, 81.

22 B. N. Figgis and J. Lewis, *Prog. Inorg. Chem.*, 1964, **6**, 37.

23 C. C. Hinckley, M. Matusz, and P. D. Robinson, *Acta Crystallogr., Sect. C*, 1988, **44**, 371.

24 S. Bucknor, F. A. Cotton, L. R. Falvello, A. H. Reid, jun., and C. D. Schmulbach, *Inorg. Chem.*, 1986, **25**, 1021.

25 F. A. Cotton, S. A. Duraj, and W. J. Roth, *Inorg. Chem*, 1984, **23**, 4046.

26 S. Al-Jibori, C. Crocker, W. S. McDonald, and B. L. Shaw, *J. Chem. Soc., Dalton Trans.*, 1981, 2589.

27 E. E. Kim, K. Eriks, and R. Magnuson, *Inorg. Chem.*, 1984, **23**, 393; K. Dehnicke, U. Müller, and R. Weber, *ibid.*, p. 2563.

28 Cambridge Structural Database, Cambridge Crystallographic Data Centre, University of Cambridge.

29 J. D. Dunitz, '*X*-Ray Analysis and the Structure of Organic Molecules,' Cornell University Press, 1979.

30 U. Müller, *Acta Crystallogr., Sect. B*, 1980, **36**, 1075 and refs. therein.

31 G. C. Allen, R. Al-Mobarak, G. A. M. El-Sharkawy, and K. D. Warren, *Inorg. Chem.*, 1972, **11**, 787.

32 A. B. P. Lever, 'Inorganic Electronic Spectroscopy,' 2nd edn., Elsevier, Amsterdam, 1984.

33 C. K. Jorgensen, *Mol. Phys.*, 1959, **2**, 309.

34 R. Greef, R. Peat, L. M. Peter, D. Pletcher, and J. Robinson, 'Instrumental Methods in Electrochemistry,' Ellis Horwood, Chichester, 1985.

35 A. Araneo and C. Bianchi, *Gazz. Chim. Ital.*, 1967, **97**, 885.

36 W. P. Griffith and D. Pawson, *J. Chem. Soc., Dalton Trans.*, 1973, 1315.

37 G. M. Sheldrick, SHELX76, Program for Crystal Structure Determination, University of Cambridge, 1976.

38 P. Roberts and G. M. Sheldrick, XANADU, Program for Crystallographic Calculations, University of Cambridge, 1979.

39 C. K. Johnson, ORTEP, Report ORNL-3794, Oak Ridge National Laboratory, Tennessee, 1965.

40 'International Tables for *X*-Ray Crystallography,' Kynoch Press, Birmingham, 1974, vol. 4, pp. 99—101.

*Received* 13*th March* 1989; *Paper* 9/01082C